Polyurethane /Ionic Silica Xerogel Composites for CO$_2$ Capture

Leonardo Moreira dos Santos[a] [ID], *Franciele Longaray Bernard[a], Ingrid Selbacch Pinto[a], Henrique Scholer[a],*

Guilherme Gerevini Dias[b] [ID], *Manoela Prado[b], Sandra Einloft[a,b]** [ID]

[a]Escola Politécnica, Pontifícia Universidade Católica do Rio Grande do Sul – PUCRS, Porto Alegre, RS, Brasil
[b]Programa de Pós-Graduação em Engenharia de Materiais e Tecnologia, Pontifícia Universidade Católica do Rio Grande do Sul – PUCRS, Porto Alegre, RS, Brasil

Capturing carbon dioxide (CO$_2$) from exhaust gases is an important strategy to prevent climate change. There is a great interest in developing novel CO$_2$ sorbents. Thus, a series of polyurethane (PU) / silica xerogels functionalized with RTILs (bmim Cl and bmim TF$_2$N) composites were prepared and characterized. PU matrix was reinforced with functionalized silica xerogels in the range of 0.5-20 wt%. PU / functionalized silica xerogels were characterized by NMR, FTIR, DSC, TGA, DMTA and FESEM. CO$_2$ sorption capacity and reusability were assessed by the pressure-decay technique at 298.15 K and 1 bar. Results showed that the filler aggregation in PU matrix promoted the reduction of mechanical properties. However, addition of silica xerogels functionalized with RTILs in PU matrix led to increased CO$_2$ uptake. CO$_2$ sorption capacity tends to increase with the incorporation of silica xerogels functionalized with RTILs in PU matrix. The best CO$_2$ sorption value was found for PU/SX-[Bmim]-[TF$_2$N] 0.5 composite (48.5 mgCO$_2$/g at 298.15 K and 1 bar). Moreover, the PU/SX-[Bmim]-[TF$_2$N] 0.5 composite showed reuse capacity and higher CO$_2$ sorption value as compared to other reported composites.

Keywords: *Ionic silica gel; polyurethane composites; CO$_2$ capture.*

1. Introduction

Increased fossil fuel energy consumption with industrial development leads to high greenhouse gas emissions (GHG)[1]. There are evidences that the increase of GHG in the atmosphere, mainly carbon dioxide (CO$_2$) resulted in climate change[1]. Carbon capture and storage (CCS) technologies are considered important strategy to both reduce CO$_2$ emission and the global warming problem[1,2]. Thus, the novel CO$_2$ sorbents synthesis are of great interest in this field[3,4].

Mixed matrix membrane (MMM) consist of a dispersed inorganic material within an organic polymer continuous matrix [5]. MMMs containing zeolitic imidazolate framework (ZIF)[6–8], silica [4,8], metal organic frameworks (MOFs) [9], nickel oxide nanoparticles[10], Zeolite [11], ZnO Nanoparticle [12], alumina nanoparticles [13], TiO$_2$ nanocomposite [14] have been studied to improve the membrane separation properties.

Inorganic particle/room-temperature ionic liquids (RTILs) composite [5,15–17] has also been examined by researchers to improve the properties of MMMs. Room temperature ionic liquids (RTILs) are salts composed by an organic cation and inorganic or organic anion presenting melting point below 100°C [18–24]. RTILs are potential solvents for CO$_2$ capture because their unique properties [22,25–29]. such as negligible vapor pressure, non-flammability, high thermal stability, tenability and selective CO$_2$ separation[19,22,23,25,27,30].

Polyurethane /silica composites have been obtained to improve polymer properties [31–37]. PU is a class of versatile polymers with potential to use in gas separation due to their low price, thermal stability, high mechanical properties and appropriate permeability[8,10]. Urethane group is the major repeating unit in PUs. However, other groups such as esters, urea, ethers and aromatic can also be present in the PU structure [38,39]. Silica incorporation into PU matrix may cause improvements in both mechanical and thermal properties, as well as gas separation properties of PU [13].

This study investigated the effect of silica xerogel functionalized with different RTILs incorporation (1-Butyl-3-Methylimidazolium Chloride - bmim Cl and 1-Butyl-3-methylimidazolium bis(trifluoromethylsulfonyl)imide - bmim TF$_2$N) on both thermal and mechanical properties, as well as CO$_2$ sorption capacity of PU.

2. Experimental

2.1 Waterborne polyurethane (WPU) synthesis

WPU synthesis was performed using experimental procedures described in literature[40,41]. Initially, polyol (MM = 1000 g/mol, Noxeller, Brasil) and dimethylol propionic acid (DMPA, 99%, Perstorp, Sweden) were charged into a five-necked flask and heated until melting. Then, 0.1% wt of dibutyltin dilaurate

(DBTDL Miracema-Nuodex Ind, Brasil) as catalyst and Isophorone diisocyanate (IPDI, Merck, USA) were poured into the same reaction flask and stirred at 80°C for 60 min to obtain NCO-terminated PU prepolymer. The NCO/OH molar ratio of 1.7 was used in the reaction. In the next step, the reaction temperature was reduced to 55°C for neutralization of carboxylic groups (-COOH) present in DMPA by adding trimethylamine (TEA, Perstorp, Sweden) (1.1 molar ratio). Finally, free NCO content (%NCO) was determined by titration with dibutylamine (Bayer, USA) and neutralized by chain extension addition in water (hydrazine, Merck, USA). The solid content of final dispersion was 35 wt%.

2.2 Silica xerogels functionalized with RTILs synthesis

Silica xerogels functionalized with RTILs were synthesized according to procedures adapted from literature[42,43]. In a typical preparation, 25 mg RTIL, 2.28 mmol TEOS (Merck, 98%, USA), PVA (Dinâmica)(4.64 g/L), NaF (Synth, 99%, Brasil) (0.20g/L) and 6.86 mmol water were mixed and cooled until gelation. The gels formed were kept at 35 °C for 1 day and washed with solvent. Finally, silica xerogels were dried at 35 °C for 1 day. The RTILs structures used in order to obtain silica xerogels are imidazolium-based ILs with two different anions as shown in Fig. 1. A silica xerogel sample (SX) was also synthesized without RTIL. Silica xerogels functionalized with RTIL were labeled as SX- RTIL. For example, SX-[bmim][Cl] means silica xerogel containing 1-Butyl-3-methylimidazolium chloride IL.
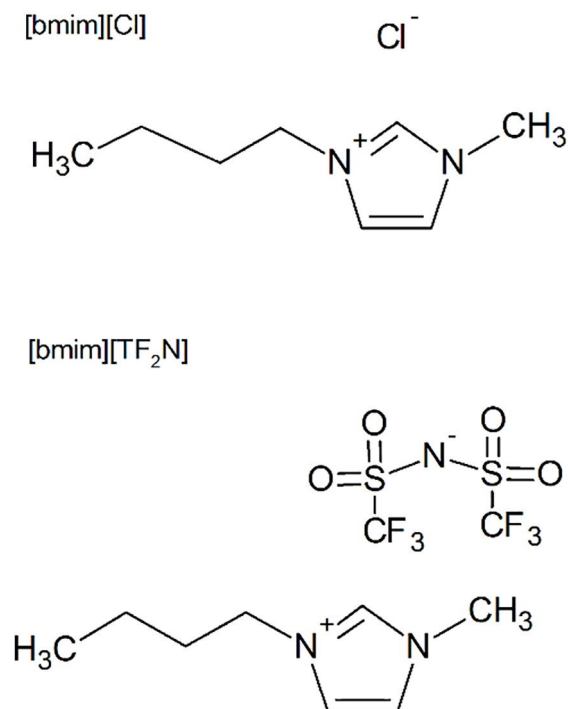

Figure 1. RTILs structures used for silica xerogels synthesis

2.3 PU composites preparation

PU/ionic silica xerogel composites were prepared by addition of silica xerogel functionalized with bmim Cl or bmim TF_2N into the WPU dispersion. PU matrix was reinforced with functionalized xerogels in the range of 0.5-20 wt% (see Table 1). In a typical preparation, mixtures were placed in ultraturrax mixer (IKA T18 Basic) during 5 min at 10,000 rpm. Finally, films around 70 μm thick were produced. The films were dried at 35 °C during 120 min.

Table 1. PU composite compositions

PU composite	Silica xerogel content (wt%)
PU/ SX-[Bmim] [Cl] 0.5	0.5
PU/SX-[Bmim] [Cl] 5	5
PU/ SX-[Bmim] [Cl] 20	20
PU/SX-[Bmim] [TF₂N] 0.5	0.5
PU/SX-[Bmim] [TF₂N] 5	5
PU/SX-[Bmim] [TF₂N] 20	20

2.4 PU composites characterization

Specific surface area, pore volume and pore *diameter* of silica xerogels were determined by Brunauer-Emmett-Teller (BET) and Barrett-Joyner-Halenda (BJH) methods, respectively using NOVA 4200e. Prior to measurements, the samples were degassed in vacuum at 125 °C for 6h. The structural elucidation of silica xerogels was carried out by solid state NMR (SS NMR) techniques. ^{13}C MAS spectra were acquired with a 7 T (300 MHz) AVANCE III Bruker spectrometer operating respectively at 75 MHz (^{13}C), equipped with a BBO probe head. The films and silica xerogels were characterized by Fourier transform infrared spectroscopy (FTIR Perkin Elmer spectrometer model Spectrum100, using UATR from 4000 at 650 cm⁻¹), 16 scans were performed for each sample and the resolution was 4. Differential Scanning Calorimetry (DSC) thermograms were attained using TA Instruments model Q20 equipment. Temperature range from -90 to 20 *°C* with a heating rate of 20 *°C* min⁻¹ was used under N₂ atmosphere. Analyses were performed in triplicate. Thermogravimetric analyses were performed using SDT equipment (TA Instruments model Q600). Temperature range was from 25 to 800 *°C* with a heating rate of 20 *°C* /min under constant N₂ flow. Analyses were performed in triplicate. Films with a thickness close to 0.15 mm, length 12 mm, and a width of approximately 7.0 mm were used to perform the stress 9 strain tests. All tests were carried out at 25 *°C* with on DMTA equipment (model Q800, TA Instruments) with 1 N/min. Young moduli of materials were determined according to procedure described elsewhere (ASTM D638).

The analyses were carried out in triplicate. Morphology of PU/ionic silica xerogel composites was investigated by field emission scanning electron microscopy (FESEM) using FEI Inspect F50 equipment in secondary electrons (SE) mode. Samples were place into a stub and covered with a thin gold layer (15-20nm).

2.5 CO$_2$ sorption measurements

CO$_2$ sorption capacity was determined using a dual-chamber gas sorption cell by pressure-decay technique previously described in detail [44–47]. Experiments were carried out in triplicate. Samples (Ws≈1g) were previously degassed under vacuum (10^{-3} mbar) at 298.15K during 1h. CO$_2$ sorption measurements were carried out at 25° C (298.15 K) and 1 Bar.

Recycle experiments were performed by repeating the sorption/desorption cycles six times at 1 bar and 25 °C (298.15 K) with desorption following each cycle under vacuum (10^{-3} mbar) at 298.15K during 1h.

3. Results and Discussion

SX-[bmim][TF$_2$N] showed higher surface area (343 m^2 g^{-1}) and pore volume (0.24 cm^3) compared to SX – [bmim] [Cl] (surface area = 116 m^2 g^{-1}, pore volume = 0.10 cm^3). However, SX – [bmim] [Cl] presented a pore diameter (1.63 nm) higher than SX-[bmim][TF$_2$N] (1.41 nm). This behavior may be related to bulky anion of [bmim][TF$_2$N] (See Fig.1) and the form as it is organized on the silica surface. ^{13}C CPMAS NMR spectra of silica xerogel are shown in Fig.2. All samples presented chemical shifts from CH$_3$, CH$_2$ and OCH$_2$ groups at 15; 29 and 57-59 ppm, respectively. SX-[bmim][TF$_2$N] and SX – [bmim] [Cl] samples showed additional chemical shifts that reveal the presence of IL, more specifically, the aromatic ring carbons at 120-130 ppm and the aliphatic chain chemical shifts between 20-40 ppm[48].
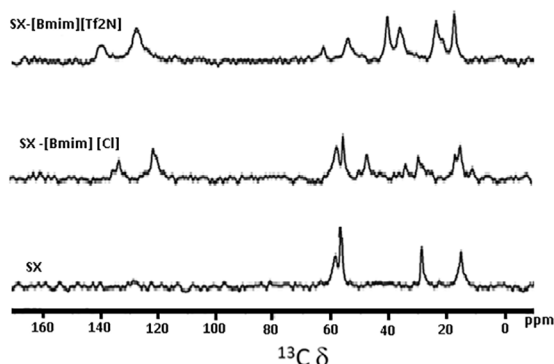

Figure 2. ^{13}C MAS spectra for silica xerogels.

FTIR analysis results for functionalized silica xerogels, PU and PU composites are shown in Fig.3 (a-b). In functionalized silica xerogels spectra revealed characteristic silica and RTIL bands at around 3305 cm^{-1} (-OH group), 1635 cm-1 (Si-OH and H-O-H), 1050 cm^{-1} (Si-O-Si) and 790 cm^{-1} (Si-O) and 1634 (C≡N imidazole)[49–51]. PU formation was observed by means of characteristic PU bands [52–54] at around 2936 - 2840 cm^{-1} (C-H), 1532 cm^{-1} (HN), 1246 cm^{-1} (C-N and C-O of urethane), 1100 cm^{-1} (C-O-C), 3350 cm^{-1} (N-H of bonded hydrogen) and 1727 cm^{-1} (C=O). FTIR analysis also showed that band area at 3322 cm^{-1} tends to increase with both the incorporation and concentration of fillers in PU matrix, indicating an increase in hydrogen bond formation in the presence of fillers [52,53,55].
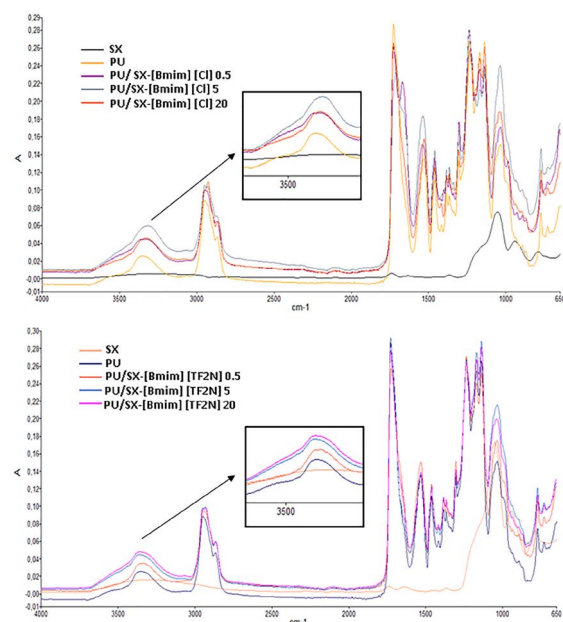

Figure 3. FTIR spectra for functionalized silica xerogels, PU and PU composites.

PU and PU composites FESEM images clearly show that fillers are unevenly dispersed in the PU matrix (Fig.4). Moreover, filler aggregation tends to increase with filler concentration increase in PU matrix. Filler aggregation in the polymer matrix may promote the reduction of mechanical properties [56,57].

PU and PU composite thermal stability was investigated by TGA. PU and PU composite TG and DTG curves are shown in Fig. 5. All samples presented three typical degradation stages (Fig.5). The first weight loss between 50°C and 150°C is related to water evaporation. The second stage is associated mainly to degradation of hard segments (urethane bonds) [58–60] and the third stage is attributed mainly to decomposition of soft segments (polyol) [61].
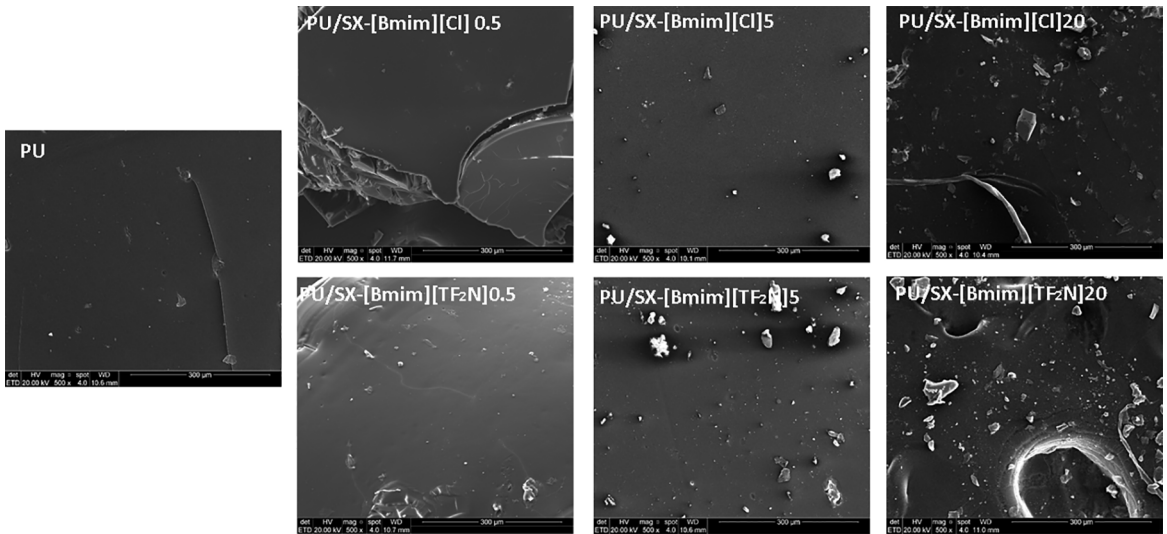
Figure 4. SEM micrographs: a) PU, b) PU/SX-[Bmim] [Cl] 0.5, c) PU/SX-[Bmim] [Cl] 5, d) PU/SX-[Bmim] [Cl] 20; e) PU/SX-[Bmim] [TF$_2$N] 0.5, f) PU/SX-[Bmim] [TF$_2$N] 5 and PU/SX-[Bmim] [TF$_2$N] 20.
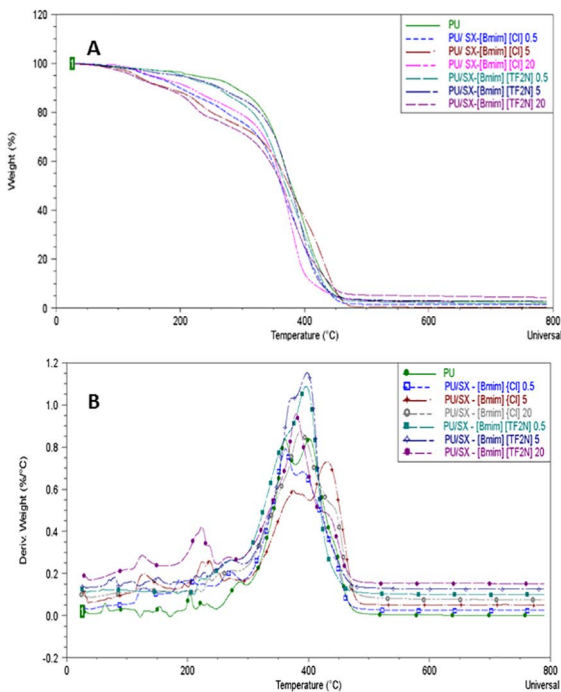

Figure 5. PU and PU composites: a) TG and b) DTG thermograms.

PU and PU composite degradation temperatures (T_{onset}) of two stages are given in Table 2. TGA analysis reveals that the addition of functionalized silica xerogels in PU matrix results in a degradation temperatures decrease (T_{onset}) as seen in Table 2. Interactions between hydroxyl groups present in the filler structure and PU hard segments can generate a deleterious effect on PU composites thermal stability. This effect might lead to breaking urethane and urea bonds of hard segments [62,63].

PU and PU composites DSC thermograms are shown in Fig. 6. PU showed a glass transition temperature (Tg) related to the soft domain at - 40.0 °C. PU composite DSC thermograms exhibited significant changes in Tg compared to PU. Tg tends to rise with filler concentration increase in PU matrix as seen in Table 2. According to these results, the hydrogen bonding increase observed by FTIR after the filler addition may be restricting the mobility of PU chains[64].

In this work, PU/SX-[Bmim] [TF$_2$N] composites were chosen to study the effects of filler addition in PU matrix on mechanical properties due to higher CO$_2$ sorption capacity compared to PU (see Fig. 7). Tensile properties and Young moduli are presented in Figs 7 and Table 3.

Table 2. TGA and DSC data for PU and PU composites

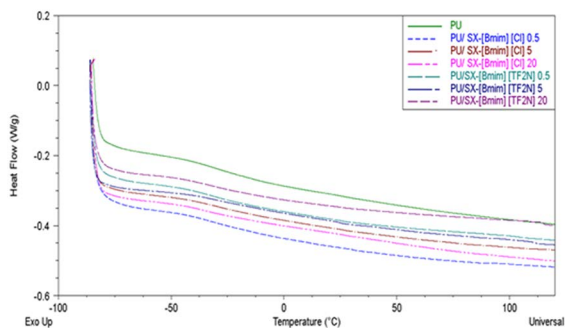| sample	$T_{1\,onset}$ (°C)	$T_{2\,onset}$ (°C)	Tg (°C)
PU	270 ± 1.2	356 ± 1.0	-40.0 ± 0.9
PU/ SX-[Bmim] [Cl] 0.5	181 ± 1.5	266 ± 1.3	-35.9 ± 0.4
PU/SX-[Bmim] [Cl] 5	194 ± 1.3	323 ± 1.0	-35.5± 0.3
PU/ SX-[Bmim] [Cl] 20	209 ± 2.0	325 ± 1.7	-30.3 ± 0.5
PU/SX-[Bmim] [TF$_2$N] 0.5	203 ± 2.2	316 ± 1.8	-35.0 ± 0.6
PU/SX-[Bmim] [TF$_2$N] 5	204 ± 0.8	320 ± 1.4	-32.9 ± 0.3
PU/SX-[Bmim] [TF$_2$N] 20	206 ± 1.3	323 ± 1.2	-30.8 ± 0.6

Figure 6. DSC thermograms obtained for PU and PU composites.

Mechanical analysis revealed that both filler addition and increased content in PU matrix results in mechanical properties reduction (See Fig.7). Young's modulus, tensile strength, elongation-at-break are decreased after filler addition in PU matrix. Thus, the best result of mechanical properties was found for PU (Young's modulus of 7.54, tensile strength of 2.41 MPa and elongation at a break of 133%). These results are consistent with FESEM finding and indicate that filler aggregates in polymer matrix promote increase of weak points in the PU composites leading to mechanical properties decrease [56,57].
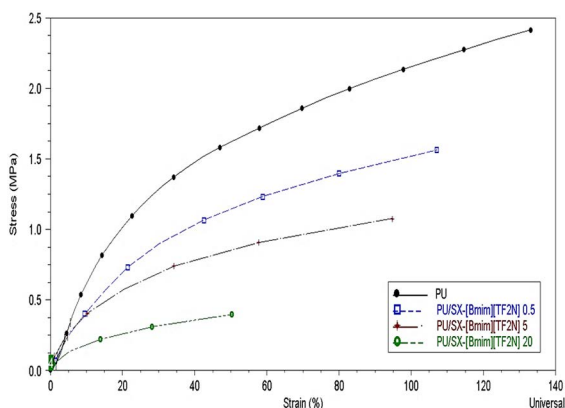

Figure 7. Stress/strain curves obtained for PU and PU composites.

CO2 sorption results are presented in Fig. 8. PU showed a CO_2 sorption capacity of 25 $mgCO_2$/g due to the polar groups present into PU structure which may promote CO_2 affinity [65,66].
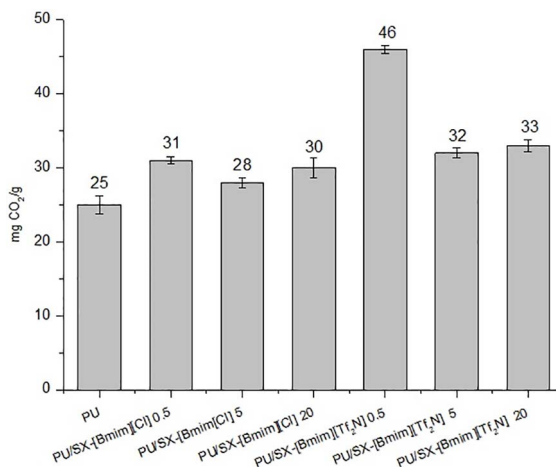

Figure 8. PU and PU composite CO_2 sorption capacity values at 0.1 bar and 298.15 K.

CO_2 sorption tends to increase with filler incorporation in PU matrix. Silica xerogel functionalization with fluorinated anion increased the affinity to CO_2 molecules compared to non-fluorinated anion (PU/ SX-[Bmim] [Cl] 0.5 = 31mgCO2/g PU/ SX-[Bmim] [TF2N] 0.5 = 46 mgCO2/g). The best CO_2 sorption values were found for PU composites prepared with SX-[Bmim] [TF2N] 0.5. This behavior is probably associated with both the higher specific surface area of SX-[Bmim] [TF2N] (343 m^2 g^{-1}) compared to SX-[Bmim] [Cl] (116 m^2 g^{-1}) and the presence of fluorinated anion that may improve CO_2 sorption [46,67]. PU/ SX-[Bmim] [Cl] CO_2 sorption values showed to be constant for all concentrations while PU/ SX-[Bmim] [TF2N] CO_2 sorption capacity tends to decrease with filler concentration increase in PU matrix possibly due to high filler aggregation in the polymer matrix evidenced by FESEM images (Fig.3). PU/SX-[Bmim] [TF2N] 0.5 composite demonstrated higher CO_2 sorption capacity (46 mgCO2/g at 298.15 K and 1 bar) as compared to reported polyvinylidene-fluoride-hexafluoropropylene (PVDF-HFP)/ amino-silica composites[4] (PVDF-HFP-20 wt% AFS = 26.27 mgCO2/g and PVDF-HFP-20 wt% ANS = 12.36 mgCO2/g at 323.15 K and 1.01 bar).

PU/SX-[Bmim] [TF2N] 0.5 was selected to recyclability study due to higher CO_2 sorption capacity compared to all other samples. CO_2 sorption capacity was increased in the first four recycles, probably due to remaining moisture.

Table 3. PU and PU composites mechanical properties

Sample	Stress (MPa)	Strain (%)	Young Moduli (MPa)
PU	2.41 ± 0.8	133 ± 0.7	7.54 ± 0.5
PU/SX-[Bmim][TF2N] 0.5	1.57 ± 0.5	107 ± 0.5	5.03 ± 0.7
PU/SX-[Bmim] [TF2N] 5	1.07 ± 0.3	94 ± 0.4	4.68 ± 0.2
PU/SX-[Bmim] [TF2N] 20	0.40 ± 0.3	50 ± 0.4	3.64 ± 0.6

CO_2 sorption values were constant for the next cycles as seen in Fig. 9. This result evidences the reuse capacity and potential of this material for use in CO_2 capture processes.
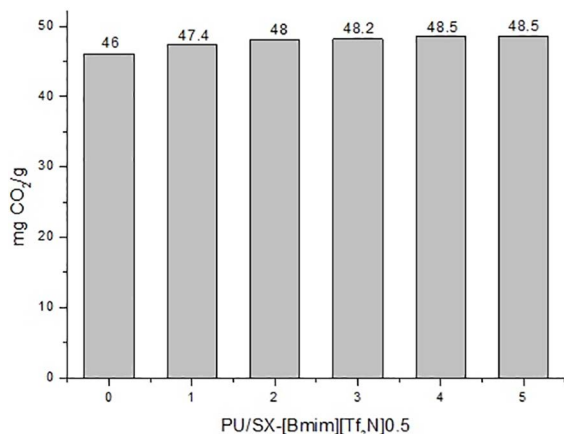

Figure 9. CO_2 sorption/desorption tests for PU/SX-[Bmim] [TF_2N] 0.5.

3. Conclusion

Uniform distribution of filler in PU matrix is desirable to obtain PU composites with improved mechanical and thermal properties. PU composites showed lower mechanical properties than PU. However, the functionalized silica xerogels addition in PU matrix led to CO_2 sorption capacity increase. CO_2 sorption values were higher for PU composites prepared from silica xerogels functionalized with fluorinated RTIL. The best CO_2 sorption capacity was found for PU/SX-[Bmim] [TF_2N] 0.5 (48.5 mgCO_2/g). Furthermore, PU composites CO_2 sorption/desorption cycle results showed both stability and reuse capacity in CO_2 capture processes.

4. Acknowledgments

5. References

1. Khan SN, Hailegiorgis SM, Man Z, Shariff AM. High pressure solubility of carbon dioxide (CO_2) in aqueous solution of piperazine (PZ) activated N-methyldiethanolamine (MDEA) solvent for CO_2 capture. *AIP Conference Proceedings*. 2017;1891(1):020081.

2. Costa CC, Melo DMA, Martinelli AE, Melo MAF, Medeiros RLBA, Marconi JA, et al. Synthesis Optimization of MCM-41 for CO_2 Adsorption Using Simplex-centroid Design. *Materials Research*. 2015;18(4):714-722.

3. Zulfiqar S, Sarwar MI, Mecerreyes D. Polymeric ionic liquids for CO_2 capture and separation: potential, progress and challenges. *Polymer Chemistry*. 2015;6(36):6435-6451.

4. Khdary NH, Abdelsalam ME. Polymer-silica nanocomposite membranes for CO_2 capturing. *Arabian Journal of Chemistry*. 2017. In Press.

5. Casado-Coterillo C, Del Mar López-Guerrero M, Irabien A. Synthesis and Characterisation of ETS-10/Acetate-based Ionic Liquid/Chitosan Mixed Matrix Membranes for CO_2/N_2 Permeation. *Membranes (Basel)*. 2014;4(2):287-301.

6. Ordoñez MJC, Balkus KJ Jr., Ferraris JP, Musselman IH. Molecular sieving realized with ZIF-8/Matrimid® mixed-matrix membranes. *Journal of Membrane Science*. 2010;361(1-2):28-37.

7. Li T, Pan Y, Peinemann KV, Lai Z. Carbon dioxide selective mixed matrix composite membrane containing ZIF-7 nano-fillers. *Journal of Membrane Science*. 2013;425-426:235-242.

8. Amedi HR, Aghajani M. Gas separation in mixed matrix membranes based on polyurethane containing SiO_2, ZSM-5, and ZIF-8 nanoparticles. *Journal of Natural Gas Science and Engineering*. 2016;35(Pt A):695-702.

9. Nik OG, Chen XY, Kaliaguine S. Functionalized metal organic framework-polyimide mixed matrix membranes for CO_2/CH_4 separation. *Journal of Membrane Science*. 2012;413-414:48-61.

10. Molki B, Aframehr WM, Bagheri R, Salimi J. Mixed matrix membranes of polyurethane with nickel oxide nanoparticles for CO_2 gas separation. *Journal of Membrane Science*. 2018;549:588-601.

11. Afarani HT, Sadeghi M, Moheb A. The Gas Separation Performance of Polyurethane-Zeolite Mixed Matrix Membranes. *Advances in Polymer Technology*. 2018;37(2):339-348.

12. Soltani B, Asghari M. Effects of ZnO Nanoparticle on the Gas Separation Performance of Polyurethane Mixed Matrix Membrane. *Membranes (Basel)*. 2017;7(3). pi:E43.

13. Ameri E, Sadeghi M, Zarei N, Pournaghshband A. Enhancement of the gas separation properties of polyurethane membranes by alumina nanoparticles. *Journal of Membrane Science*. 2015;479:11-19.

14. Sadeghi M, Afarani HT, Tarashi Z. Preparation and investigation of the gas separation properties of polyurethane-TiO_2 nanocomposite membranes. *Korean Journal of Chemical Engineering*. 2015;32(1):97-103.

15. Hao L, Li P, Yang T, Chung TS. Room temperature ionic liquid/ZIF-8 mixed-matrix membranes for natural gas sweetening and post-combustion CO_2 capture. *Journal of Membrane Science*. 2013;436:221-231.

16. Rynkowska E, Fatyeyeva K, Kujawski W. Application of polymer-based membranes containing ionic liquids in membrane separation processes: a critical review. *Reviews in Chemical Engineering*. 2018;34(3):341-363.

17. Hudiono YC, Carlisle TK, Bara JE, Zhang Y, Gin DL, Noble RD. A three-component mixed-matrix membrane with enhanced CO_2 separation properties based on zeolites and ionic liquid materials. *Journal of Membrane Science*. 2010;350(1-2):117-123.

18. Wilkes JS. A short history of ionic liquids - from molten salts to neoteric solvents. *Green Chemistry*. 2002;4(2):73-80.

19. Figueroa JD, Fout T, Plasynski S, McIlvried H, Srivastava RD. Advances in CO₂ capture technology—The U.S. Department of Energy's Carbon Sequestration Program. *International Journal of Greenhouse Gas Control*. 2008;2(1):9-20.

20. Xue Z, Zhang Z, Han J, Chen Y, Mu T. Carbon dioxide capture by a dual amino ionic liquid with amino-functionalized imidazolium cation and taurine anion. *International Journal of Greenhouse Gas Control*. 2011;5(4):628-633.

21. Tomé LC, Marrucho IM. Ionic liquid-based materials: a platform to design engineered CO₂ separation membranes. *Chemical Society Reviews*. 2016;45(10):2785-2824.

22. Privalova EI, Mäki-Arvela P, Murzin DY, Mikkhola JP. Capturing CO₂: conventional versus ionic-liquid based technologies. *Russian Chemical Reviews*. 2012;81(5):435.

23. Dai Z, Noble RD, Gin DL, Zhang X, Deng L. Combination of ionic liquids with membrane technology: A new approach for CO₂ separation. *Journal of Membrane Science*. 2016;497:1-20.

24. Paolone A, Palumbo O, Trequattrini F, Appetecchi GB. Relaxational Dynamics in the PYR₁₄-IM₁₄ Ionic Liquid by Mechanical Spectroscopy. *Materials Research*. 2018;21(Suppl 2):e20170870.

25. Kenarsari SD, Yang D, Jiang G, Zhang S, Wang J, Russell AG, et al. Review of recent advances in carbon dioxide separation and capture. *RSC Advances*. 2013;3(45):22739-22773.

26. Sadeghpour M, Yusoff R, Aroua MK. Polymeric ionic liquids (PILs) for CO₂ capture. *Reviews in Chemical Engineering*. 2017;33(2):183-200.

27. Brennecke JF, Gurkan BE. Ionic Liquids for CO₂ Capture and Emission Reduction. *The Journal of Physical Chemistry Letters*. 2010;1(24):3459-3464.

28. Markewitz P, Kuckshinrichs W, Leitner W, Linssen J, Zapp P, Bongartz R, et al. Worldwide innovations in the development of carbon capture technologies and the utilization of CO₂. *Energy and Environmental Science*. 2012;5(6):7281-7305.

29. Ketzer JM, Iglesias RS, Einloft S. Reducing Greenhouse Gas Emissions with CO₂ Capture and Geological Storage. In: Lackner M, Chen WY, Suzuki T, eds. *Handbook of Climate Change Mitigation and Adaptation*. 2nd ed. New York: Springer. p. 1-40.

30. Hasib-ur-Rahman M, Siaj M, Larachi F. Ionic liquids for CO₂ capture—Development and progress. *Chemical Engineering and Processing: Process Intensification*. 2010;49(4):313-322.

31. Chen Y, Zhou S, Yang H, Wu L. Structure and properties of polyurethane/nanosilica composites. *Journal of Applied Polymer Science*. 2005;95(5):1032-1039.

32. Chung YC, Chung KH, Choi JW, Chun BC. Preparation of hybrid polyurethane–silica composites by a lateral sol-gel process using tetraethyl orthosilicate. *Journal of Composite Materials*. 2018;52(2):159-168.

33. Jang MK, Lee SK, Kim BK. Polyurethane nano-composite with functionalized silica particle. *Composite Interfaces*. 2008;15(6):549-559.

34. Dourbash A, Buratti C, Belloni E, Motahari S. Preparation and characterization of polyurethane/silica aerogel nanocomposite materials. *Journal of Applied Polymer Science*. 2017;134(8):44521.

35. Petrović ZS, Javni I, Waddon A, Bánhegyi G. Structure and properties of polyurethane-silica nanocomposites. *Journal of Applied Polymer Science*. 2000;76(2):133-151.

36. Yang G, Liu X, Lipik V. Evaluation of silica aerogel-reinforced polyurethane foams for footwear applications. *Journal of Membrane Science*. 2018;53(13):9463-9472.

37. Sá e Sant'Anna S, de Souza DA, de Araujo DM, Carvalho CF, Yoshida MI. Physico-chemical analysis of flexible polyurethane foams containing commercial calcium carbonate. *Materials Research*. 2008;11(4):433-438.

38. Akindoyo JO, Beg MDH, Ghazali S, Islam MR, Jeyaratnam N, Yuvaraj AR. Polyurethane types, synthesis and applications – a review. *RSC Advances*. 2016;6(115):114453-114482.

39. Chattopadhyay DK, Webster DC. Thermal stability and flame retardancy of polyurethanes. *Progress in Polymer Science*. 2009;34(10):1068-1133.

40. Soares RR, Carone C, Einloft S, Ligabue R, Monteiro WF. Synthesis and characterization of waterborne polyurethane/ZnO composites. *Polymer Bulletin*. 2014;71(4):829-838.

41. dos Santos LM, Ligabue R, Dumas A, Le Roux C, Micoud P, Meunier JF, et al. Waterborne polyurethane/Fe₃O₄-synthetic talc composites: synthesis, characterization, and magnetic properties. *Polymer Bulletin*. 2018;75(5):1915-1930.

42. Vidinha P, Augusto V, Almeida M, Fonseca I, Fidalgo A, Ilharco L, et al. Sol–gel encapsulation: An efficient and versatile immobilization technique for cutinase in non-aqueous media. *Journal of Biotechnology*. 2006;121(1):23-33.

43. Vidinha P, Augusto V, Nunes J, Lima JC, Cabral JM, Barreiros S. Probing the microenvironment of sol–gel entrapped cutinase: The role of added zeolite NaY. *Journal of Biotechnology*. 2008;135(2):181-189.

44. Fernández Rojas M, Pacheco Miranda L, Martinez Ramirez A, Pradilla Quintero K, Bernard F, Einloft S, et al. New biocomposites based on castor oil polyurethane foams and ionic liquids for CO₂ capture. *Fluid Phase Equilibria*. 2017;452:103-112.

45. Azimi A, Mirzaei M. Experimental evaluation and thermodynamic modeling of hydrate selectivity in separation of CO₂ and CH₄. *Chemical Engineering Research and Design*. 2016;111:262-268.

46. Duczinski R, Bernard F, Rojas M, Duarte E, Chaban V, Dalla Vecchia F, et al. Waste derived MCMRH- supported IL for CO₂/CH₄ separation. *Journal of Natural Gas Science and Engineering*. 2018;54:54-64.

47. Campbell S, Bernard FL, Rodrigues DM, Rojas MF, Carreño LA, Chaban VV, et al. Performance of metal-functionalized rice husk cellulose for CO₂ sorption and CO₂/N₂ separation. *Fuel*. 2019;239:737-746.

48. Corvo MC, Sardinha J, Casimiro T, Marin G, Seferin M, Einloft S, et al. A Rational Approach to CO₂ Capture by Imidazolium Ionic Liquids: Tuning CO₂ Solubility by Cation Alkyl Branching. *ChemSusChem*. 2015;8(11):1935-1946.

49. Mor S, Manchanda CK, Kansal SK, Ravindra K. Nanosilica extraction from processed agricultural residue using green technology. *Journal of Cleaner Production*. 2017;143:1284-1290.

50. Shirini F, Mazloumi M, Seddighi M. Acidic ionic liquid immobilized on nanoporous Na^+-montmorillonite as an efficient and reusable catalyst for the formylation of amines and alcohols. *Research on Chemical Intermediates*. 2016;42(3):1759-1776.

51. Huang X, Li W, Wang M, Tan X, Wang Q, Zhang M, et al. Synthesis of multiple-shelled organosilica hollow nanospheres via a dual-template method by using compressed CO_2. *Microporous and Mesoporous Materials*. 2017;247:66-74.

52. Coleman MM, Lee KH, Skrovanek DJ, Painter PC. Hydrogen bonding in polymers. 4. Infrared temperature studies of a simple polyurethane. *Macromolecules*. 1986;19(8):2149-2157.

53. Zhang M, Hemp ST, Zhang M, Allen MH Jr., Carmean RN, Moore RB, et al. Water-dispersible cationic polyurethanes containing pendant trialkylphosphoniums. *Polymer Chemistry*. 2014;5(12):3795-3803.

54. Lee HT, Wu SY, Jeng RJ. Effects of sulfonated polyol on the properties of the resultant aqueous polyurethane dispersions. *Colloids and Surfaces A: Physicochemical and Engineering Aspects*. 2006;276(1-3):176-185.

55. Bernard FL, Polesso BB, Cobalchini FW, Donato AJ, Seferin M, Ligabue R, et al. CO_2 capture: Tuning cation-anion interaction in urethane based poly(ionic liquids). *Polymer*. 2016;102:199-208.

56. Wang HH, Chen KV. A novel synthesis of reactive nano-clay polyurethane and its physical and dyeing properties. *Journal of Applied Polymer Science*. 2007;105(3):1581-1590.

57. Hassanajili S, Sajedi MT. Fumed silica/polyurethane nanocomposites: effect of silica concentration and its surface modification on rheology and mechanical properties. *Iranian Polymer Journal*. 2016;25(8):697-710.

58. Cervantes-Uc JM, Moo Espinosa JI, Cauich-Rodríguez JV, Ávila-Ortega A, Vázquez-Torres H, Marcos-Fernández A, et al. TGA/FTIR studies of segmented aliphatic polyurethanes and their nanocomposites prepared with commercial montmorillonites. *Polymer Degradation and Stability*. 2009;94(10):1666-1677.

59. Petrović ZS, Zavargo Z, Flyn JH, Macknight WJ. Thermal degradation of segmented polyurethanes. *Journal of Applied Polymer Science*. 1994;51(6):1087-1095.

60. Barikani M, Fazeli N, Barikani M. Study on thermal properties of polyurethane-urea elastomers prepared with different dianiline chain extenders. *Journal of Polymer Engineering*. 2013;33(1):87-94.

61. Pashaei S, Siddaramaiah, Syed AA. Thermal Degradation Kinetics of Polyurethane/Organically Modified Montmorillonite Clay Nanocomposites by TGA. *Journal of Macromolecular Science, Part A: Pure and Applied Chemistry*. 2010;47(8):777-783.

62. Ma XY, Zhang WD. Effects of flower-like ZnO nanowhiskers on the mechanical, thermal and antibacterial properties of waterborne polyurethane. *Polymer Degradation and Stability*. 2009;94(7):1103-1109.

63. Dias G, Prado M, Le Roux C, Poirier M, Micoud P, Ligabue R, et al. Analyzing the influence of different synthetic talcs in waterborne polyurethane nanocomposites obtainment. *Journal of Applied Polymer Science*. 2018;135(14):46107.

64. Meera KMS, Sankar RM, Paul J, Jaisankar SN, Mandal AB. The influence of applied silica nanoparticles on a bio-renewable castor oil based polyurethane nanocomposite and its physicochemical properties. *Physical Chemistry Chemical Physics*. 2014;16(20):9276-9288.

65. Tomasko DL, Li H, Liu D, Han X, Wingert MJ, Lee LJ, et al. Koelling. A Review of CO_2 Applications in the Processing of Polymers. *Industrial & Engineering Chemistry Research*. 2003;42(25):6431-6456.

66. Gabrienko AA, Ewing AV, Chibiryaev AM, Agafontsev AM, Dubkov KA, Kazarian SG. New insights into the mechanism of interaction between CO_2 and polymers from thermodynamic parameters obtained by *in situ* ATR-FTIR spectroscopy. *Physical Chemistry Chemical Physics*. 2016;18(9):6465-6475.

67. Blanchard LA, Gu Z, Brennecke JF. High-Pressure Phase Behavior of Ionic Liquid/CO_2 Systems. *The Journal of Physical Chemistry B*. 2001;105(12):2437-2444.